



# Environmental Sustainability Analysis of a Hybrid Heat Source Dryer

N. R. Nwakuba<sup>1</sup> · M. C. Ndukwu<sup>2</sup> · G. U. Asonye<sup>1</sup> · S. N. Asoegwu<sup>1</sup> · G. I. Nwandikom<sup>1</sup>

Received: 8 March 2020 / Revised: 4 August 2020 / Accepted: 15 October 2020 / Published online: 1 November 2020  
© Escola Politécnica - Universidade de São Paulo 2020

## Abstract

This paper presents the energy and exergy-based environmental sustainability analyses of a developed solar dryer equipped with electric heater as supplementary heat. The experimental study was applied for drying a local variety of red pepper (*Shombo*) near a coastal region of eastern Nigeria. The objectives of the study were to assess the suitability and overall performances of the hybrid solar dryer in this area. Results obtained indicate that the solar collector contributed about 39.4 to 48.5% of the total drying air temperature required for drying operation. The energy efficiency of the hybrid solar dryer ranged between 13.2 to 35.6%, whereas the specific energy requirements varied between 7.24 kJkg<sup>-1</sup> to 63.5 kJkg<sup>-1</sup>. The percent solar energy contribution to the total energy requirement ranged between 28.8–52.68% at varying air temperatures (50, 60, and 70°C) and air velocities (1.14, 2.29, and 3.43 ms<sup>-1</sup>). The drying time varied between 75 ± 5 to 180 ± 24 min. The energy and exergy efficiencies varied between 13.2–35.6% and 35.8 to 92.3%, respectively. The exergy-based sustainability indicators which take into account the ratio of waste exergy, sustainability index, and improvement capacity of the hybrid heat source dryer were found to be 0.11–0.167, 1.14–6.12, and 0.099–0.289 kJs<sup>-1</sup>, respectively. Comparison between a CI-engine powered dryer reveals that the use of a hybrid solar-electric dryer can prevent emission of 398.86 to 3872.7 tons of CO<sub>2</sub> into the environment per annum. Recommendation for future studies was suggested.

**Keywords** Energy-exergy · Electric heat · Solar radiation · Hybrid dryer · Environment · Sustainability

## 1 Introduction

Given the rapid depletion of petroleum resources all over the world and certain apprehension about it because of the role petroleum products play in global climatic change, renewable energy resources have been explored as a replacement (Nwajinka and Onuegbu 2014; Maia et al. 2017). In the case of drying purposes, solar dryers are being applied in place of conventional fossil-based dryers (Reyes et al. 2014; Nwakuba et al. 2016; Maia et al. 2017). They are environmentally friendly and economically worthwhile especially in developing countries (Amer et al. 2010; Lamidi et al. 2019). Nigeria is a tropical

country, with seasonally damp and humid weather variation during the year, especially within locations closer to the coast. However, its daily sunshine duration varies between 3.5 hours in the south to 9 hours towards the Sahel region (Nwakuba et al. 2020; Uzoma et al. 2020). Therefore, this beneficially placed it to harness considerable amount of solar energy for plant-based thermal processing and other energy applications.

Open sun drying has remained the preferred method for drying of crops in many tropical and sub-tropical regions due to its economic benefits, irrespective of its limitations (Okoroigwe et al. 2013; Silva et al. 2020). Unfortunately, this method exposes the dried product to dirt and other animal incursions. However, in southern part of Nigeria closer to the Atlantic Ocean, the intermittent nature of solar radiation as well as frequent dilution of sunshine period (inter-tropical discontinuity) and precipitation have limited the application of solar drying application for crop drying (Hossain et al. 2018; El-Ferouali et al. 2019; Nwakuba et al. 2020). To solve this problem, researchers are adopting hybrid systems that incorporate other heat sources such as electricity or biomass heater to supplement for the solar energy during off sun-shine

✉ N. R. Nwakuba  
nnaemeka.nwakuba@futo.edu.ng

<sup>1</sup> Department of Agricultural and Bioresources Engineering, Federal University of Technology, Owerri, Nigeria

<sup>2</sup> Department of Agricultural and Bioresources Engineering, Michael Okpara University of Agriculture, Umudike, Nigeria

periods (El-Ferouali et al. 2019; Lamrani et al., 2019; Nwakuba et al. 2020; Silva et al. 2020). It permits continued drying operation during off-sunshine hours to prevent rewetting which prolongs the drying time and exposes the product to microbial attack (Amer et al. 2010; Nwakuba et al. 2017). The use of electricity as a feasible supplementary energy font for solar drying systems has been reported by several researchers (Alejandro et al. 2013; Amer et al. 2018; El-Ferouali et al. 2019; Silava et al. 2020). Apart from the ease of usage, non-polluting characteristics and high heat density, supplementing solar drying with electricity provides a strategy to lower the overall energy cost for drying and carbon emission if conventional energy is to be continuously used for the same purpose. Additionally, amongst all the unit operations involved in crop processing, drying operation is considered to be the most energy intensive because of the elevated  $h_{fg}$ -value of water and unproductive heat transfer by the air stream (Aghbashlo et al. 2013; Nwakuba et al. 2020). Thus, any strategy that will reduce the cost of energy to enhance dryer efficiency for good quality dried food products is encouraged by food processors (Aghbashlo et al. 2013; Aviara et al. 2014; Shamekhi-Amiri et al. 2018).

As a result of excessive energy intake of drying operation, one of the major interests to crop dryers is how to conserve energy. Great emphasis is placed on efficient energy utilization for drying (Nwakuba et al. 2018). Therefore, researchers have carried out energy-based performance analyses to estimate different processes to conserve energy; evaluate quantitatively energy needs of a drying system (Aviara et al. 2014). However, this method provides a serious challenge as it does not identify the various losses that occur within the system; thus, the quality of the final energy is not known. Therefore, exergy analysis which takes into consideration various losses within the system has become a more useful tool for performing energy evaluations (Aghbashlo et al. 2013). Exergy analysis has also amongst its advantages the ability to present the environmental sustainability impact of energy utilization (Erbay and Icier 2011; Nazghelich et al. 2010; Aghbashlo et al. 2013; Aviara et al. 2014; Ndukwu et al. 2018a). This latter part is becoming of interest to researchers due to climate issues. Processes involving energy utilization leads to waste of energy to the environment. This waste energy can be dangerous like in the case of solar radiation; it can lead to re-radiation of the solar radiation (Dincer and Rosen 2013). In recent years, sustainability analyses based on exergy evaluation as well as drying system optimization have become an interesting area amongst researchers (Aghbashlo et al. 2013; Ndukwu et al. 2017; Sansaniwal et al. 2018). According to Ndukwu et al. (2017), sustainability entails energy supply at lesser damage to the environment. Therefore, understanding of sustainability will prevent ecological damage (Rosen et al. 2008; Ndukwu et al. 2020a).

Although some research has been carried out on hybrid solar dryers in Nigeria and some other tropical countries; however, analysis of these dryers focused on drying kinetics of the products and time reduction abilities (Boughali et al. 2009; Ndukwu et al. 2018a). This present study considers the performance of hybrid solar dryers in relation to varying operational factors viz, temperature of air, speed of air, and sample thickness, which some researchers (Aghbashlo et al. 2013; Aviara et al. 2014; Ndukwu et al. 2018a, b; Ndukwu et al. 2020b) did not put into consideration. Very few papers reported the efficiency of solar and hybrid solar drying systems as well as their environmental sustainability and improvement potentials based on their exergy streams. Even those that reported the efficiencies adopted two methods which include energy and exergy flow of air mass (Fudholi et al. 2016; Ndukwu et al. 2017; Castro et al. 2018), and dynamic model approach: in which the varying product temperatures and moisture contents were taken into cognizance (Hatami et al. 2019; Ndukwu et al. 2020a). The results obtained from these two approaches varied mainly as a result of structural design, mode of heat supply, and type of product handled. Irrespective of the approach adopted, available scientific studies which focused more on solar drying systems, showed that results obtained are both system, environmental, and crop specific. A few literature was found on hybrid solar-biomass dryers (Nwofe 2014; Borah et al. 2017; Ndukwu et al. 2018b; Ndukwu et al. 2020a). Currently there is no available research on the concurrent energy-exergy and environmental sustainability study of an electric-assisted solar dryers for Nigerian indigenous crops like, *shombo* red pepper. This paper therefore, focuses on energy and exergy-based thermodynamic evaluations and environmental sustainability study of a solar dryer furnished with electric heater, in humid Nigerian region. The obtained data will assist in system modeling and optimization of the developed hybrid solar dryer.

## 2 Materials and Methods

### 2.1 Sample Set Up

An indigenous specie of garden-fresh red pepper (*Shombo*) with initial moisture content of 81.94% wet basis (w.b) was procured from an open market in Owerri capital city of Imo State-Nigeria for the experimental analysis (Fig. 1). For each batch of drying run, 0.5 kg of fully red coloured samples were sliced into thicknesses of 10 mm, 15 mm, and 20 mm by making use of a fruit slicing device and a digital venire calipre (precision  $\pm 0.05$  mm). The samples were sliced perpendicular to the vertical axis (Fig. 1). The mean initial moisture content of the *Shombo* pepper products was determined gravimetrically by oven-drying 20 g representative sample at 105°C for 24



**Fig. 1** a Garden-fresh *shombo* red pepper samples; b Sliced pepper samples for convective drying

hours (Scientico M55 model, India) (Darvishi et al. 2013; Nwakuba et al. 2020; Uzoma et al. 2020).

## 2.2 Dryer System Description and Experimental Procedure

The prototype hybrid heat source dryer, HHSD (Fig. 2) consisted of three major units namely: air heater units (solar collector and electrical resistance wire), drying compartment (with two stratum of wire-mesh rack), and microprocessor (Arduino, version C++, SPK16.000G). Table 1 demonstrates the technical descriptions of HHSD components. The solar collector ( $95 \times 70 \times 20 \text{ cm}^3$ ) is made of 1.5 cm thick fiber glass sandwiched by plywood and covered with transparent plain glass. The collector was tilted  $15.54^\circ$  northwards, with its absorber made with 1 mm thick steel plate and painted black. In order to deliver the desired amount of drying air to evacuate moist air, the solar collector in-flow air was channeled into the drying chamber through a cuboid-shaped hood lagged with 1.5 cm thick-layer of kaolin. To provide for supplementary electric heating, a resistance wire of 1500 W, was mounted at right angle to the flow track of the incoming air at the exit-end of the

collector to form a hybrid unit. The auxiliary electric unit automatically switches on when the temperature of air in the drying compartment falls (1 deg. C) below the set drying temperature to augment the drying air temperature.

The compartment for drying which measures:  $45 \times 45 \times 50 \text{ cm}^3$ , was made with a laminated board coated with 3 cm thick kaolin. Two square drying racks ( $40 \times 40 \text{ cm}^2$ ) made of plastic netting were suspended on an analogue-type weighing balance (Camry model, China) connected to a mass sensor (Trans\_tech, China  $\pm 0.001 \text{ g}$ ). The air temperature and relative humidity sensors were stationed at five separate spots on the dryer (inlet-port, collector, upper and lower drying racks, and chimney) and linked to the microprocessor which measures the readings and displays them on a computer screen. An axial fan was placed in the chimney, mounted on the hood of the drying chamber. The axial fan and microprocessors were powered by an 80 W, 12 V photovoltaic cell via a 2.5 kVA inverter and 12 V DC accumulator.

Before the beginning of the actual experiment which took place in the peak of rainy season (known for low irradiation period and excessive air humidity), the dryer was operated using the absorbed solar flux by the solar air-collector unit in order to ascertain its level of heat generation and/or contribution. The ambient air velocity, air-temperature, relative

**Fig. 2** Pictorial view of the hybrid heat source dryer arrangement



**Table 1** Technical specifics of the hybrid dryer components

S/N	Component	Rating/model
1.	Photovoltaic cell	80 W, 12 V
2.	Accumulator	75 Amps., 12 V
3.	Plain glass	4 mm thick; dim: $92 \times 67 \times 17 \text{ cm}^3$
4.	Solar air-collector	NBF laminated board ( $95 \times 70 \times 20 \text{ cm}^3$ )
5.	Resistance wire	Cu: 1500 W, 240 V, 50 Hz.
6.	Absorber sheet	1 mm steel sheet ( $93.5 \times 68.5 \times 18.5 \text{ cm}^3$ )
7.	Frame support	Angle iron
8.	Rollers	2 cm diameter, rubber rollers
9.	Inverter system	2.5 kVA, 50 Hz
10.	Relays and contactor	30 Amps and 2 hp, respectively

humidity, solar air-collector temperature and relative humidity, and solar irradiation were measured to ascertain the thermal performance of the solar collector. The temperature, flow rate of air, plus relative humidity of air were measured with a high sensitive thermocouple, digital anemometer, and electronic hygrometer, respectively. Actual experimental tests were conducted by positioning the HHSD in the open and measurement of amount of incident solar radiation on the solar collector was performed hourly with an Apogee-pyranometer. Three levels of air temperatures (50, 60, and 70°C) and air rates of flow (1.14, 2.29, and 3.43  $\text{ms}^{-1}$ ) were selected based on the range of prevailing ambient air flow rates. The mass of the sliced pepper samples was recorded at 30-minutes intervals to compute the moisture loss. Each drying batch was terminated when the samples attained a mass loss corresponding to  $10 \pm 1\%$  w.b. (Tiwari 2012; Nwakuba et al. 2020). Response surface (3-D) plots were used in analyzing the specific energy requirements and drying time of the samples as affected by the operational variables.

### 2.2.1 Energy Study

The total useful energy used for drying a batch of red pepper slices by the hybrid system is the aggregate of the heat generated by the solar collector and electrical resistance wire expressed as Eq. (1):

$$Q_u = Q_{sc} + Q_e \quad (1)$$

Lopez-Vidana et al. (2013) and Ndukwu et al. (2017) expressed  $Q_{sc}$  as:

$$Q_{sc} = A_{sc} F_R [(\alpha\tau) - U_1(T_{sc} - T_a)] \quad (2)$$

$$F_R = \frac{M_a C_{pa}}{U_1 A_{sc}} \left[ 1 - e^{\frac{-A_{sc} U_1 F'}{M_a C_{pa}}} \right] \quad (3)$$

Where:  $Q_u$ ,  $Q_{sc}$  and  $Q_e$  represent the total useful energy used, solar collector useful heat generated, and electric

heat, respectively (kJ);  $F_R$  is the heat removal parameter;  $A_{sc}$  is the solar collector area ( $\text{m}^2$ );  $\alpha\tau$  is effective transmittance-absorbance of glass;  $T_{sc}$  and  $T_a$  are temperatures of solar collector temperature and atmospheric air, respectively ( $^{\circ}\text{C}$ );  $V_a$  is the air velocity in the solar collector ( $\text{m/s}$ );  $C_{pa}$  is the specific heat capacity of air;  $F'$  is the efficiency factor (decimal) while  $U_1$  is the overall thermal loss ( $\text{Wm}^{-2}$ ) given as the summation of the heat energy lost through the top, bottom, and sides of the solar air-collector ( $U_t$ ,  $U_b$ , and  $U_s$ , respectively), expressed in Eq. (4) as:

$$U_1 = U_t + U_b + U_s \quad (4)$$

$$Q_e = \left( \frac{H_p A_h}{L_h} \right) t \quad (5)$$

Where:  $H_p$  is the heater rated power,  $A_h$  is the heater area,  $L_h$  is the heater length,  $t$  is drying time (s).

The specific energy requirement ( $E_{sp}$ ) is expressed as Eq. (6) (Beigi 2016; Nwakuba et al. 2018; Nwakuba et al. 2020):

$$E_{sp} = Q_u / M_m \quad (6)$$

Where:  $M_m$  is amount of lost sample moisture (kg).

The solar collector efficiency, defined as the ratio of solar energy output to the solar energy input to the collector, was calculated using Eq. (7) (Lopez-Vidana et al. 2013; Fudholi et al. 2016):

$$\eta_{sc} = \frac{V_a C_{pa} (T_o - T_i)}{I_g A_{sc}} \quad (7)$$

Where:  $\eta_{sc}$  is the solar collector efficiency (%);  $T_o$  and  $T_i$  are the solar collector output and input air temperatures, respectively ( $^{\circ}\text{C}$ );  $I_g$  is the mean irradiance on the solar air-collector ( $\text{Wm}^{-2}$ ).

The drying efficiency of a hybrid solar-electric dryer, is given as (Boughali et al. 2009; Fudholi et al. 2016):

$$\eta_d = \frac{M_m L}{A_{sc} I_g + F_p + \left( \frac{Q_e}{t} \right)} \quad (8)$$

Where:  $\eta_d$  is the dryer efficiency (%),  $L$  is the heat of moisture evaporation ( $\text{kJkg}^{-1}$ ),  $F_p$  is the fan power (4 W).

The first law of thermodynamics was applied in calculating the energy utilization ratio ( $\dot{E}_u$ ), termed as the fraction of energy utilized for moisture desorption to energy supplied by the hybrid heat source, and was determined as expressed in Eq. (9) (Aviara et al. 2014):

$$\dot{E}_u = M_a \left( \frac{h_{a1} - h_{a2}}{h_{a1} - h_a} \right) \quad (9)$$

Where:  $h_a$  is the enthalpy of the ambient dry air ( $\text{kJkg}^{-1}$ ).

The energy efficiency refers to the proportion of energy exhausted during drying to the energy supplied by the heat sources is expressed as Eq. (10):

$$\eta_e = \frac{E_1 - E_2}{E_1} = \frac{M_a(h_{a1} - h_{a2})}{M_a h_{a1}} \times 100 \tag{10}$$

Where:  $\eta_e$  is the energy efficiency (%);  $E_1$  and  $E_2$  are the entry and exit energy variables, respectively (kJ).

### 2.2.2 Exergy Study

The concept of the 2nd law of heat-dynamics was applied in analyzing the exergetic performance of the hybrid solar dryer, since the actual drying process is characterized by energy quality deficit (Ndukwu et al. 2017). The exergetic examination of the hybrid drying course was categorized into: exergy study of the solar collector unit and exergy study of the combined solar and electric thermal units (hybrid). For an open system, the exergy balance is expressed using the characteristics of the drying air. It has the internal energy, entropic, work, momentum, gravity, chemical and radiation emission components as expressed in Eq. (11) (Aviara et al. 2014; Ndukwu et al. 2017; Ndukwu et al. 2020a, b, c):

$$\begin{aligned} E_X = & (U - U_\infty) + T_\infty(S - S_\infty) + \frac{P_\infty}{J}(V - V_\infty) \\ & + \frac{V^2}{2gJ} + (Z - Z_\infty) \frac{g}{g_c J} + V(P - P_\infty) \\ & + \sum_c (U_0 - U_\infty) N_c \\ & + E_1 A_1 F_1 (3T^4 - T_\infty^4 - 4T_\infty T^3) \end{aligned} \tag{11}$$

Where:  $E_x$  is the exergy of the drying process ( $\text{kJkg}^{-1}$ ); the subscripts:  $\infty$ ,  $c$ , and  $1$  represent reference or ambient condition, chemical and inlet, respectively;  $T_\infty$  is the ambient temperature ( $^\circ\text{C}$ );  $N$  is the number of species;  $F$  is the shape factor;  $A$  is the area ( $\text{m}^2$ );  $T$  is the absolute air temperature (K);  $V$  is the air velocity ( $\text{ms}^{-1}$ );  $U$  is the internal energy ( $\text{kJkg}^{-1}$ );  $E$  is the emissive power ( $\text{kJ}^{-1}$ );  $P$  is the pressure (kPa);  $S$  is the specific entropy ( $\text{kJkg}^{-1}$ ).

The general expression for exergy stream applicable to hybrid solar-electric dryer during sunshine hours (Eq. 12) was developed by considering the flow of electric current and diffusional flow. The enthalpy for the internal energy and PV-terms related systems of steady flow were substituted into Eq. (11) to yield Eq. (12) under the conditions of neglected momentum, gravity and chemical components, plus pressure variations in the drying system, since  $V \cong V_\infty$  (Aviara et al. 2014; Ndukwu et al. 2017).

$$E_X = M_a C_{pa} \left[ (T_d - T_a) - T_a \ln \frac{T_d}{T_a} \right] \tag{12}$$

Where:  $T_d$  and  $T_a$  are the drying chamber temperature and ambient temperature, respectively ( $^\circ\text{C}$ ).

Since drying operation was done only with the hybrid mode, the exergy loss (lost work potential) of the drying process can be obtained based on the entry and exit air temperatures of the drying compartment, expressed as Eq. (13):

$$\sum E_{Xl} = \sum E_{Xi} - \sum E_{Xo} \tag{13}$$

Where:  $E_{Xl}$  = exergy loss ( $\text{kJ}^{-1}$ );  $E_{Xi}$  and  $E_{Xo}$  are entry and exit exergy flow rates, respectively ( $\text{kJ}^{-1}$ ).

Eqs. (14) and (15) describe the entry and exit exergy flow of the drying compartment and rack, respectively as:

$$E_{XD_i} = E_{Xr_i} = M_a C_p \left[ (T_{Di} - T_a) - T_a \ln \frac{T_{Di}}{T_a} \right] \tag{14}$$

$$E_{XD_o} = E_{Xr_o} = M_a C_p \left[ (T_{Do} - T_a) - T_a \ln \frac{T_{Do}}{T_a} \right] \tag{15}$$

Where:  $E_{XD_i}$  and  $E_{XD_o}$  = entry and exit exergy of the drying compartment, respectively ( $\text{kJ}^{-1}$ ),  $E_{Xr_i}$  and  $E_{Xr_o}$  = entry and exit exergy of the drying rack, respectively ( $\text{kJ}^{-1}$ ),  $T_{Di}$  and  $T_{Do}$  are entry and exit temperatures of the drying compartment, respectively ( $^\circ\text{C}$ ).

The exergy efficiency ( $\eta_{E_X}$ ) of the hybrid system is imperative in defining the actual performance of the crop dryer. The exergy efficiency of a hybrid solar-electric drying system is given by Eq. (16) (Fudholi et al. 2016):

$$\eta_{E_X} = \frac{E_{XD_o}}{E_{XD_i}} = 1 - \frac{E_{Xl}}{E_{XD_i}} \tag{16}$$

### 2.2.3 Sustainability Indices

The quest for incorporation of ecological aspects into renewable energy scheduling for sustainable advancement introduced different exergy sustainability indicators. Some researchers observed that exergy sustainability of drying process varies with air temperature and air velocity (Midilli and Kucuk 2014; Ndukwu et al. 2017; Fu et al. 2018). This work considers the following exergy sustainability indicators for hybrid solar drying obtained using Eqs. (17) to (19), respectively. They are: improvement potential ( $P_{im}$ ), waste-exergy ratio ( $E_w$ ) and sustainability index ( $S^n$ ).

$$E_w = \frac{E_{Xl}}{E_{Xi}} \tag{17}$$

$$S^n = \frac{1}{1 - \eta_{E_X}} \tag{18}$$

$$P_{im} = (1 - \eta_{E_X}) E_{Xl} \tag{19}$$

### 2.3 Environmental Effect

Comparison of the energy use of the hybrid heat source dryer (HHSD) with a compression ignition (CI) engine-operated crop dryer was made. The energy production of the CI gen-set is computed by Eq. (20) (Ould-Amrouche et al. 2010; Ndukwu et al. 2020a, b, c):

$$Q_u = \beta_c \cdot h_v \cdot \mathcal{D}_v \equiv Q_{sc} + Q_e = \beta_c \cdot h_v \cdot \mathcal{D}_v \tag{20}$$

Where:  $\beta_c$  = conversion efficiency of a 5 kW CI generator (0.299–0.353%),  $h_v$  = heating value of diesel (10.08 kWhl<sup>-1</sup>),  $\mathcal{D}_v$  = volume of diesel consumed (litres), as stated by Ould-Amrouche et al. (2010).

The quantity of diesel required to generate equal amount of heat by HHSD for drying a batch of red pepper slices is calculated thus:

$$\mathcal{D}_v = \frac{Q_u}{\beta_c \cdot h_v} \tag{21}$$

The exhaust quantity of CO<sub>2</sub> ( $\mathbb{V}_c$ ) per liter of diesel is estimated as (Ndukwu et al. 2017):

$$\mathbb{V}_c = \beta_c \cdot h_v \tag{22}$$

Where:  $W_c$  = equivalent weight of CO<sub>2</sub> (2.63 kg l<sup>-1</sup>).

The quantity of CO<sub>2</sub> emission drop ( $\epsilon_{CO_2}$ ) is estimated in terms of rate of HHSD usage as (Ould-Amrouche et al. 2010; Ndukwu et al. 2017):

$$\epsilon_{CO_2} = A_p \cdot \mathbb{V}_c \tag{23}$$

Where:  $Y_p$  = Yearly percent period of operation of HHSD (10 ≤  $Y_p$  ≤ 100%) (Ndukwu et al. 2020a, b, c).

Yearly cost of diesel consumption,  $Y_d$  (\$), assuming a working period of the CI engine-powered dryer of 240 days year<sup>-1</sup> (Ould-Amrouche et al. 2010; Nwakuba et al. 2020):

$$Y_d = 365 D_c \mathcal{D}_v \tag{24}$$

Where:  $D_c$  is the mean price of diesel fuel in Nigeria (0.787 \$m<sup>-3</sup>); 1 USD ≡ 305.8, 1 litre = 240.52 NGN as at 2017.

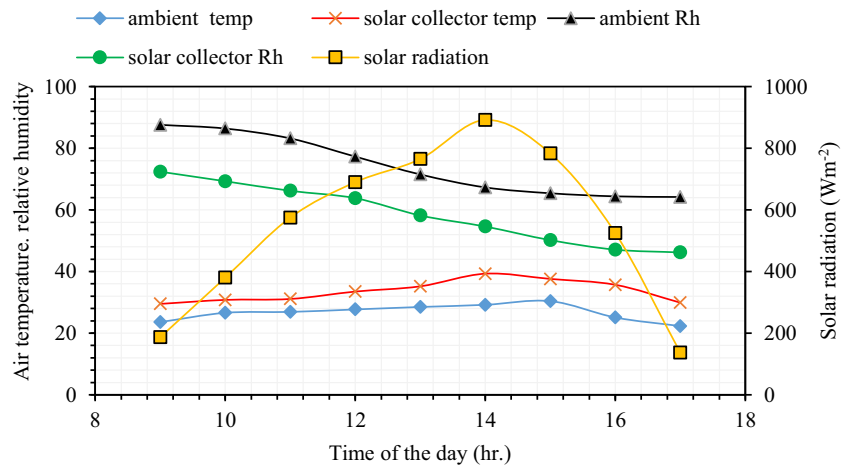
## 3 Results and Discussion

### 3.1 Solar Collector Performances

Figure 3 depicts the hourly variations of ambient condition during the drying period. The mean solar collector temperatures were higher than the ambient by approximately 15%, which indicates the suitability of the solar collector as associate heat source for drying purposes. The percent rise in the solar collector temperature is as a result of the early insolation at the emergence of bright sky, which was used to enhance the enthalpy of the collector inlet air thus, warming-up the collector as the marginal temperature increase is insufficient for moisture diffusion in the red pepper samples. Ndukwu et al. (2018b) and Ndukwu et al. (2020a) reported similar observation for hybrid solar dryers. They noted that early insolation from 5 am – 8 am pre-heats the collector and causes minimal moisture content reduction in the red pepper samples.

The peak solar collector temperature of 39.3°C was obtained at 14:00 hrs and this occurred one hour before the peak ambient temperature was reached. The collector relative humidity varied with the intensity of solar flux. A comparable pattern was seen in the experimental results of Nwajinka and Onuegbu (2014); Ndukwu et al. (2017); Nwakuba et al. (2017); Jamil and Bellos (2019). The prevalent high ambient relative humidity which reduces with increasing hourly time, inversely affects the solar collector temperature. The relative humidity of the solar collector was observed to be lesser than the ambient and both decreased with increasing solar intensity which increased the enthalpy of the solar collector. The

**Fig. 3** Average air temperature, relative humidity, and incident solar radiation



thermal performance of the solar collector as well as the amount of solar heat contribution to the hybrid system are functions of the solar intensity. The obtained solar intensity ranged from  $187 \text{ Wm}^{-2}$  to  $892 \text{ Wm}^{-2}$  throughout the drying periods for all air velocities. Within this range of solar intensity, the efficiency of the solar collector fluctuated between 23.7–72.4% and, with a mean value of 40.6%. This efficiency varied proportionally with irradiation concentration during the drying period as displayed in Fig. 4. Similar results were obtained by Bennamoun (2012); Fudholi et al. (2016); Hossain et al. (2018); Nwakuba et al. (2020).

### 3.2 Energy Utilization

The extent of energy utilized ( $E_u$ ) for drying of red pepper slices in the HHSD at variable air temperatures, air velocities, and thicknesses of slice is presented in Fig. 5. At constant airflow rate, greater amount of energy was consumed at rising temperature which caused further moisture removal in thicker samples due to increased enthalpy of drying air, thus increased  $E_u$ . Considering thickness of slice,  $E_u$ -value intensified with thicker slices at constant air temperature and airflow rate.

Increasing the airflow rate increases the heat transfer rate, thus more energy is utilized. More moisture is evaporated from the sample surface at constant slice thickness, as a result of increased distance of moisture transport, hence more energy is utilized. Similar findings have been documented in the research of Aghbashlo et al. (2008); Nazghelichi et al. (2010); Beigi (2016); Azadbakht et al. (2017); Nwakuba et al. (2018) for potato slices, carrot slices, apple slices, eggplant slices and okra slices, respectively. The  $E_u$ -value for red pepper slices varied between  $176.95 \text{ Js}^{-1}$ – $3273.66 \text{ Js}^{-1}$ , at drying temperatures of  $50^\circ\text{C}$ – $70^\circ\text{C}$ , slice thicknesses of 10–20 mm and air velocities of  $1.14$ – $3.43 \text{ ms}^{-1}$ . Similar results were reported on potato slices in a mini industrial-type continuous-band dryer eggplant slices in a fluidized bed dryer, ball pepper in an electric dryer, sliced tomatoes in a hybrid solar-electric dryer

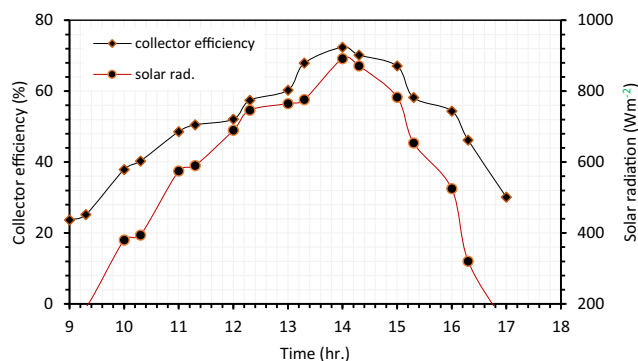


**Fig. 4** Change in mean solar collector efficiency and solar radiation with hourly time

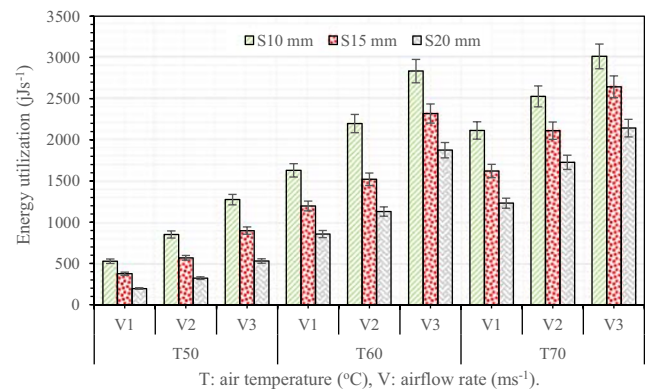


**Fig. 5** Energy utilization at varying drying variables

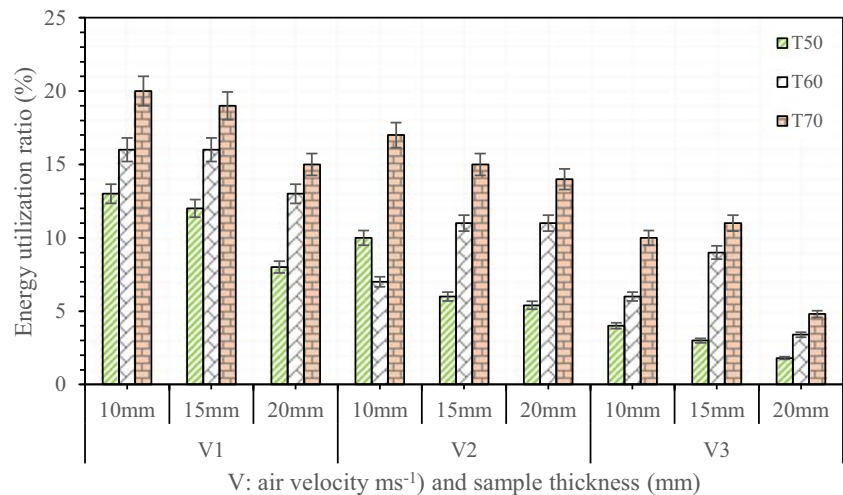
(Akpınar 2004; Aghbashlo et al. 2008; Azadbakht et al. 2017; Nwakuba et al. 2020).

The effect of varying drying variables on energy utilization ratio ( $\dot{E}_u$ ) during of the pepper slices is presented in Fig. 6. With rising temperature of air, the  $\dot{E}_u$ -values increased, but diminished with higher rate of air flow. Similar results on the effects of varying drying air temperatures, slice thicknesses and air velocity on  $\dot{E}_u$  have been reported by other studies for drying biomaterials (Nwakuba et al. 2020; Uzoma et al. 2020).

Increasing the sample thickness at constant temperature and flow of drying air decreases  $\dot{E}_u$  values because of short thermal gradient between the sample matrix and the hot moving air which results in gross reduction in moisture removal rate, thus the input energy becomes unable to penetrate the sample and initiate moisture diffusion. The  $\dot{E}_u$  values varied between 1.82–20.4% for all drying condition which indicates that the energy utilized from the hybrid heat source was efficiently used for drying of red pepper slices at high air temperature. Generally, reducing sample thickness at increased air temperature and decreasing air velocity yielded high energy utilization ratio. The  $\dot{E}_u$  parameter therefore, seems to be veritable for analyzing energy utilization during thin-layer drying operations. Azadbakht et al. (2017) suggest that low  $\dot{E}_u$  at varying drying conditions indicate availability of energy in the exiting drying air, which when recovered could grossly upsurge the energy efficiency of the drying machine.

The  $\eta_c$ -value (Fig. 7) reveals a rising trend in the efficiency of energy usage (13.2 to 35.6%) for drying of red pepper slices in a hybrid solar dryer increased from 13.2 to 35.6% as temperature and slice thickness increase from  $50$  to  $70^\circ\text{C}$  and 10 to 20 mm, respectively at constant air velocity. This value is within the range reported by Aviara et al. (2014) and Beigi (2016) on the convective drying of cassava starch and

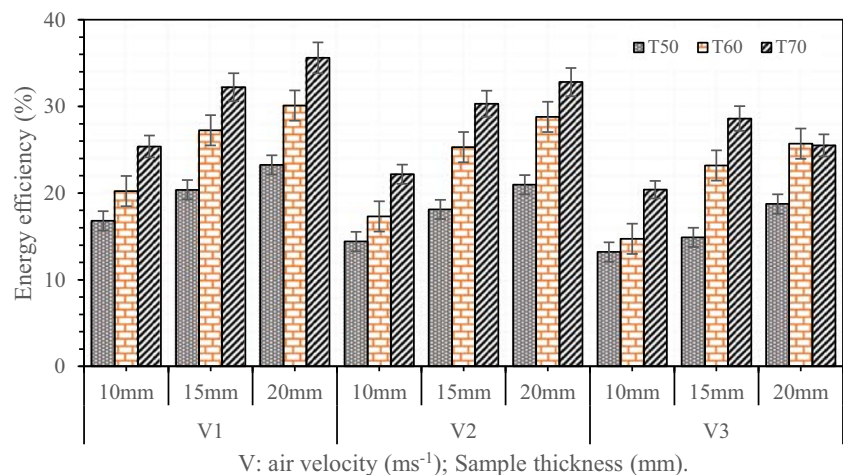
**Fig. 6** Energy utilization ratio at varying drying variables



sliced-apples, respectively. Chowdhury et al. (2011) also reported similar energy efficiency on solar drying jackfruit leather. The highest and lowest energy efficiency values were established at  $70^{\circ}\text{C}$ ,  $1.14\text{ ms}^{-1}$ , 20 mm and  $50^{\circ}\text{C}$ ,  $3.43\text{ ms}^{-1}$ , 10 mm, respectively.

The effects of the drying variables on the specific energy requirements are presented in Fig. 8a-c. Increasing the drying air temperature at decreasing slice thickness requires less amount of specific energy. This is as a result of increased thermal gradient between the drying air and the sample products which lessened the drying time, thus reduction in specific energy requirement. Increasing the temperature and air flow reduces the specific energy requirement due to increased heat transfer rate and water pressure deficit in the sliced samples. Upsurge in the rate of air flow reduces the specific energy requirement due to increased heat and moisture transfer rates at constant air temperature. The maximum ( $63.5\text{ kJkg}^{-1}$ ) and minimum ( $7.24\text{ kJkg}^{-1}$ ) specific energy requirements were obtained at drying parameters of  $50^{\circ}\text{C}$ ,  $2.29\text{ ms}^{-1}$ , 20 mm and  $60^{\circ}\text{C}$ ,  $3.43\text{ ms}^{-1}$ , 10 mm, respectively.

**Fig. 7** Energy efficiency of HHSD at different with temperatures, airflow rates and thickness levels



### 3.3 Energy Support of the Solar Collector

The energy backing of the collector (Table 2) was estimated by subtracting the electrical energy consumed from the total energy intake of HHSD. Higher preset air temperature at regular airflow decreases the collector's energy contribution as a result of greater heat density of the electrical heater and the large thermal gradient between the collector outlet air temperature and the drying compartment preset air temperature, whereas higher airflow at regular drying temperature boosts the percent solar energy contribution. The solar energy contribution to the total energy consumption varied between 28.8–52.68%. From the energy perspective, this design of hybrid solar dryer prefers drying operation at air velocity of relatively high percent solar energy consumption. This enhances the drying efficiency, reduces drying time, in addition to the total energy utilization.



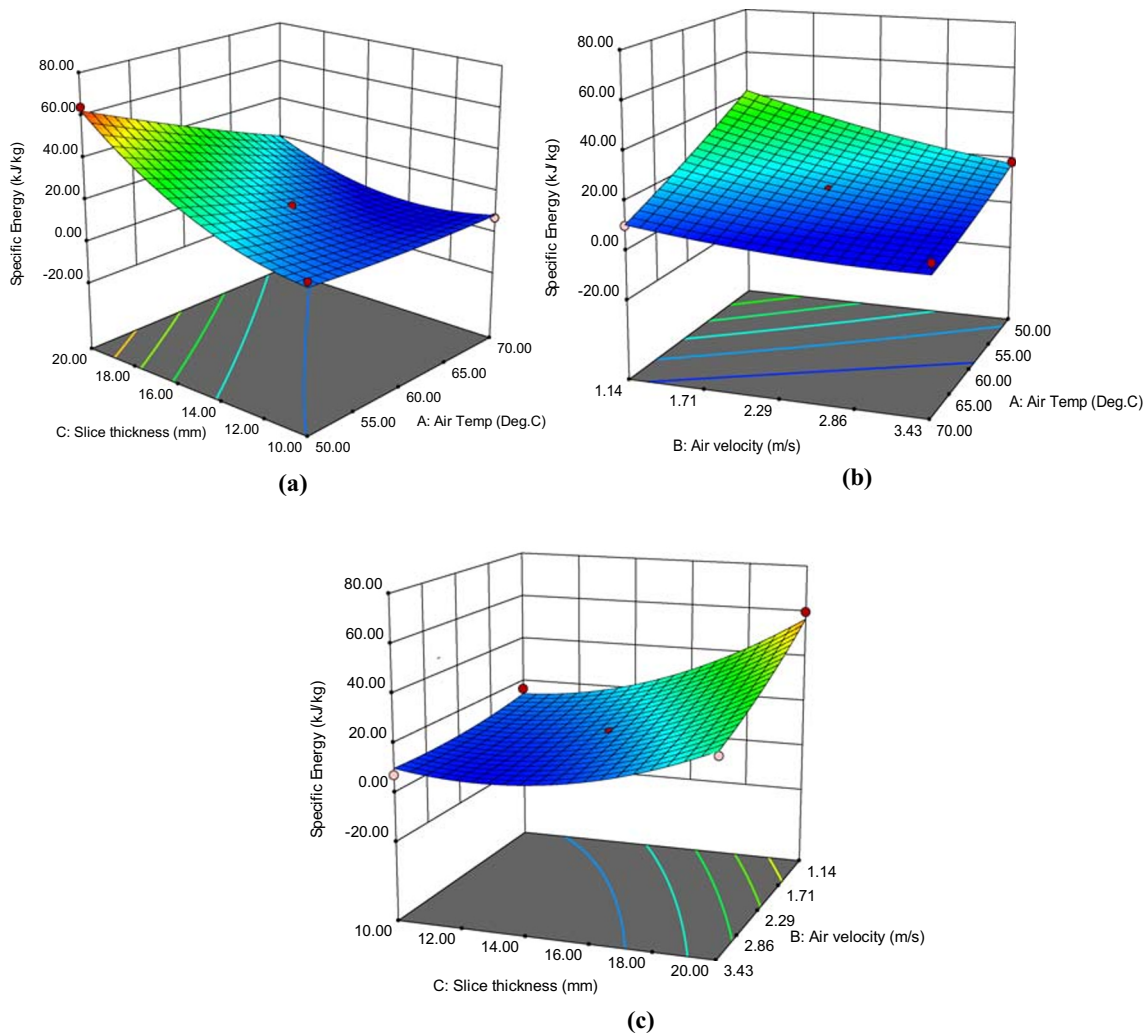


**Fig. 8** Variation of specific energy requirements with: **a** air temperature and slice thickness; **b** air temperature and air velocity; **c** air velocity and slice thickness

### 3.4 Drying Kinetics

The proportion of moisture release to the drying air at constant flow rate tends to reduce with rise in temperature of air (Fig. 9). It is evident that as the drying temperature increases, drying time shortens because of internal energy gain by sample moisture for speedy capillary flow and from the sample matrix. Therefore, the drying kinetics exhibited the nonexistence of the constant drying rate phase of the sample product. This suggests that moisture capillary flow is the most likely

physical mechanism regulating the transfer of mass in the drying samples. This is in conformity with the research outcomes of Motevali et al. (2012), for drying of jujube fruits;

**Table 2** Energy contributions of solar collector to the hybrid dryer

Air velocity ( $\text{ms}^{-1}$ )	Percent solar energy consumed (%)		
	50°C	60°C	70°C
1.14	41.93	35.64	28.87
2.29	48.90	40.10	32.88
3.43	52.68	44.25	37.44

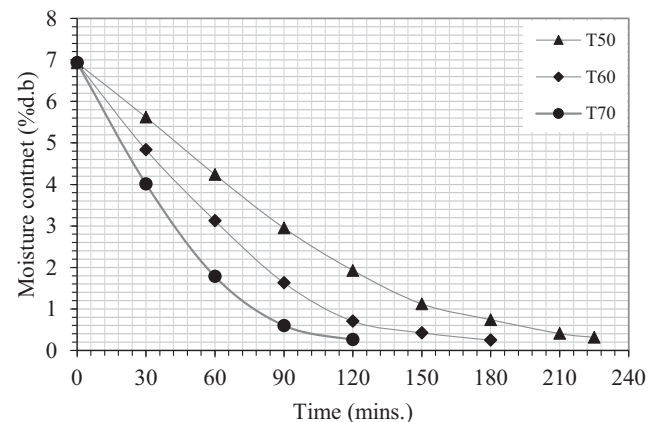


**Fig. 9** Time of drying as affected by moisture content of red pepper slices

Afolabi et al. (2014) in drying of ginger slices; Doymaz (2004) for carrot slices, respectively.

Higher air temperatures and air flow at constant thickness of slice reduces the drying time because of increase in evaporation rate of surface moisture, hence quicker drying process (Fig. 10a). During this period, vapour pressure deficit occurred within the product matrix with less resistance to moisture release at a higher rate. The reports of Motevali et al. (2012) and Minaei et al. (2014) corroborated this observation; whereas increasing the slice thickness increases the drying time due to increased capillary distance of the sample matrix (Fig. 10b). Increasing the air velocity intensifies the transference rate of heat that enhances the drying rate, thereby reducing the drying time (Fig. 10c). The maximum and minimum drying times of red pepper slices were found to be  $180 \pm 24$  min to  $75 \pm 5$  min, respectively at drying conditions of  $50^\circ\text{C}$ , 20 mm,  $3.43 \text{ ms}^{-1}$  and  $70^\circ\text{C}$ , 10 mm,  $1.14 \text{ ms}^{-1}$ , respectively.

### 3.5 Exergy Performance

#### 3.5.1 Exergy of the Solar Collector

The mean exergy flow of the solar collector was observed to be dependent upon the varying hourly time. The interaction effect between mean solar radiation and the mean entry, exit, and lost exergy of the solar collector is shown in Fig. 11. The exergy flow increased with time and peaked at time range of 12:00–13:00 hours and began to decrease as the solar radiation decreases. Similar observation was recorded by Akpınar (2011) in drying of parsley leaves using solar cabinet dryer. High exergy loss of the solar collector was observed at 12:00 hours and reduced as the Sun sets. This is an indication of increased solar flux and inlet drying air temperature which is predicated by the lost exergy. The entry, exit, and lost exergy of the collector ranged between  $0.019$  and  $0.674 \text{ kJs}^{-1}$ ,  $0.016$ – $0.351 \text{ kJs}^{-1}$  and  $0.003$ – $0.0345 \text{ kJs}^{-1}$ , respectively.

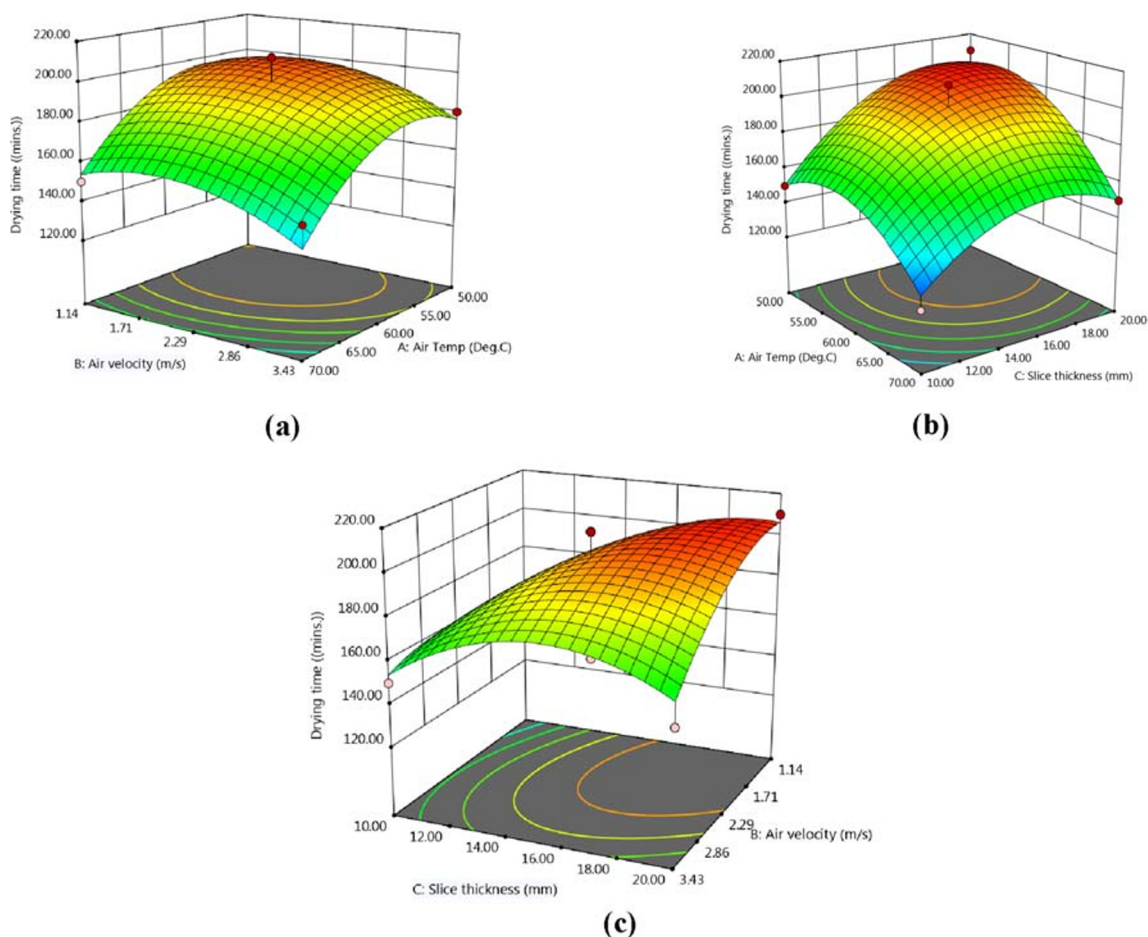


**Fig. 10** Change in the time of red pepper drying with: **a** temperature and air flow; **b** air temperature and slice thickness; **c** slice thickness and air flow

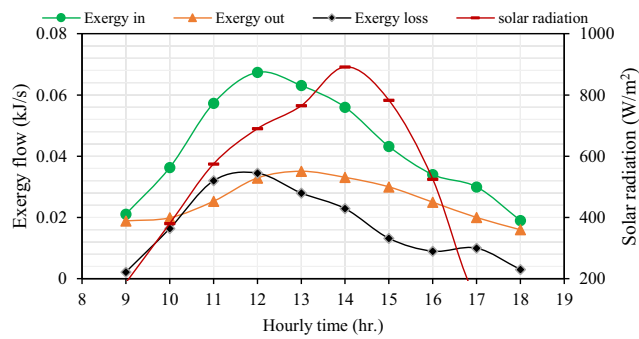


**Fig. 11** Effect of hourly time and mean solar radiation on the mean exergy flow of the solar collector

### 3.5.2 Exergy of Red Pepper Drying

The mean exergy inflow and outflow obtained at variable speeds of air and drying temperatures are given in Table 3. The entry and exit exergy of the drying compartment increased with drying air temperature at increasing air velocity. The exergy inflow to the drying chamber varied between 3.194 – 10.01 kJs<sup>-1</sup> for the range of the studied drying air temperature. Related outcomes were documented by Akpınar (2004); Aghbaslo et al. (2008); Azadbakht et al. (2017).

The maximum exergy loss (1.295 kJs<sup>-1</sup>) was obtained at 70°C air temperature and 3.43 ms<sup>-1</sup> air velocity. This shows that a larger amount of exergy delivered to the drying compartment was efficiently exploited for drying of pepper slices. Whereas the minimum exergy loss (0.327 kJs<sup>-1</sup>) was obtained at 50°C air temperature and 1.41 ms<sup>-1</sup> air velocity; implying that a little fraction of exergy inflow was utilized for drying. Nevertheless, these exergy values show that lesser quantity of exergy was utilized and there is substantial quantity of energy available in the exiting air as shown in Table 3.

### 3.5.3 Exergy Efficiency

The varying exergy efficiencies of HHSD with air temperature and air flow rate at varying slice thicknesses of the sample are shown in Fig. 12. The  $\eta_{E_x}$  -values decreased with higher values of air temperature as a result of substantial increase in exergy loss. Also, since exergy efficiency varies inversely with exergy rate of drying air. This observation conforms to the findings of Aghbaslo et al. (2013). Furthermore, increasing the air flow decreases  $\eta_{E_x}$  as a result of increased loss of exergy from the drying chamber. This exergy loss played a critical part in lessening  $\eta_{E_x}$  of the drying compartment through temperature upturn and velocity of air (Aghbaslo et al. 2013; Eltawil et al. 2018). Increased inlet drying air temperature (with higher exergy) causes increase in product moisture diffusion and surface evaporation and exergy utilization; hence increased exergy loss. However, reduction in  $\eta_{E_x}$  of the drying compartment was prompted by the energy supplied by the solar collector and electric resistance wire were productively used for drying process. These results also establish that  $\eta_{E_x}$  was improved by increasing the sample thickness.

The highest exergy efficiency of 89.6% was attained at 50°C, 1.14 ms<sup>-1</sup> and 20 mm drying variables; whereas the least value of exergy efficiency (35.8%) was obtained at 70°C 3.43 ms<sup>-1</sup> and 10 mm. At constant 60°C temperature, exergy efficiency was highest with the lowest airflow (1.14 ms<sup>-1</sup>) for the range of studied sample thickness. These values signify that the exergy outflow of the hybrid dryer is a major parameter of thermodynamic inadequacy, indicating further that a considerable amount of thermal exergy delivered to the system was lost to the exhaust air (Chenga et al. 2018). This is also an indication of a marginal shortfall in the design of the dryer configuration, vis-à-vis the location and sizing of the heating units. Therefore, in a bid to enrich the drying system thermodynamic efficiency and lower the exergy loss,

**Table 3** Mean exergy inflow and outflow at varying air velocities and drying air temperatures and constant slice thickness (10 mm)

Drying air temperature (°C)	Air velocity (ms <sup>-1</sup> )								
	1.14			2.29			3.43		
	Exergy inflow (kJ/s <sup>-1</sup> )	Exergy outflow (kJ/s <sup>-1</sup> )	Exergy loss (kJ/s <sup>-1</sup> )	Exergy inflow (kJ/s <sup>-1</sup> )	Exergy outflow (kJ/s <sup>-1</sup> )	Exergy loss (kJ/s <sup>-1</sup> )	Exerg (kJ/s <sup>-1</sup> ) y inflow (kJ/s <sup>-1</sup> )	Exergy outflow (kJ/s <sup>-1</sup> )	Exergy loss (kJ/s <sup>-1</sup> )
50	3.194	2.867	0.327	5.217	4.735	0.482	7.321	6.561	0.760
60	4.131	3.715	0.416	6.311	5.711	0.600	8.106	7.135	0.971
70	6.145	5.626	0.519	7.016	6.172	0.844	10.01	8.715	1.295

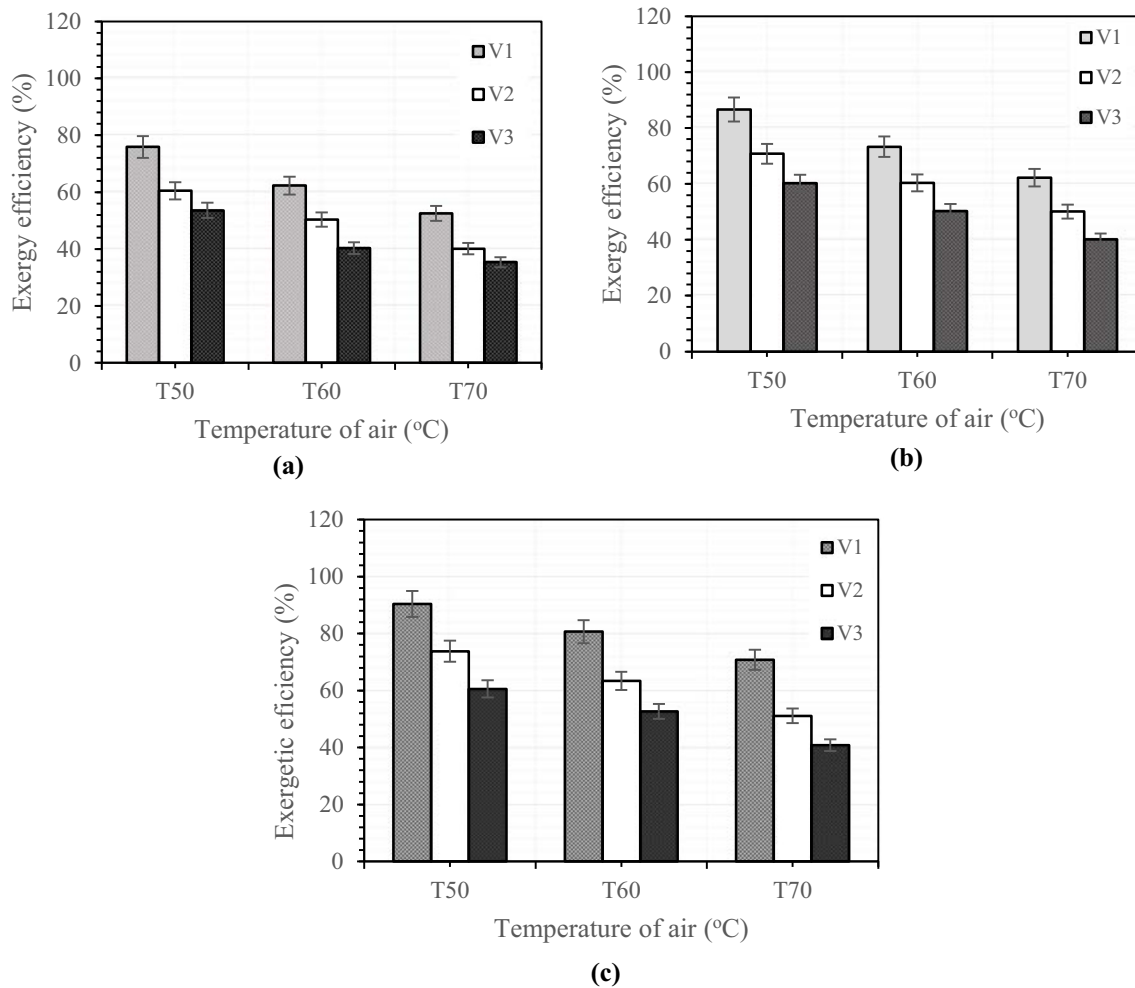


**Fig. 12** Exergy efficiency of HHSD as affected by temperature and air flow at: (a) 10 mm, (b) 15 mm and (c) 20 mm slice thicknesses

recycling of the lost exergy through heat recovery units and tube-like heat exchangers, proper lagging of the heating and drying chambers (with layers of drying racks) as well as optimizing the drying conditions and pre-heating the inflow air would bring hope toward reducing the exergy loss and improving the system's thermodynamic efficiency (Cheng et al. 2018; Eltawil et al. 2018). The optimization result however, would help in adequate sizing of the supplementary heat source located within the dryer plenum.

### 3.6 Sustainability Parameters

Analyses of exergy stream of a system illustrates the association between energy flows and environmental sustainability (Nwakuba et al. 2020). The consequences of environmental sustainability is evident in the quantity of lost exergy. This has the potential of affecting the survival of the ecosystem inhabitants as well as mode of utilization of resources (Dincer and Rosen 2013, Ndukwu et al. 2020a, b, c). Figures 13, 14 and 15 therefore, present the results of exergy sustainability indicators of HHSD. In an attempt to improve the inlet temperature

above the ambient level and increase the moisture removal capacity of the air stream as well as moisture differential for rapid diffusion and overall crop drying purposes, the drying chamber lost some amount of exergy to the exhaust air. This exergy loss when compared to the inflow exergy of the drying

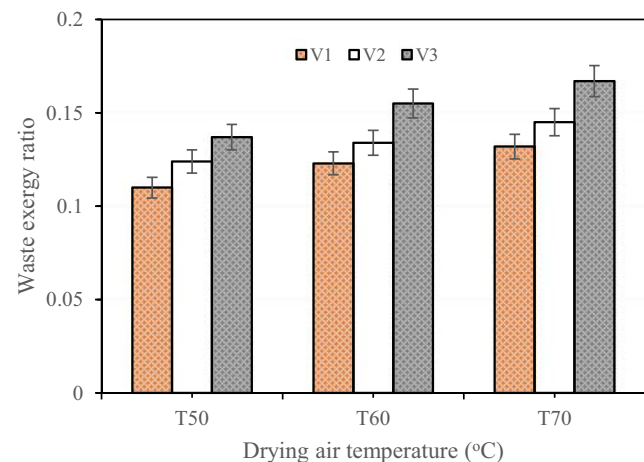


**Fig. 13** Waste exergy ratio of red pepper in HHSD

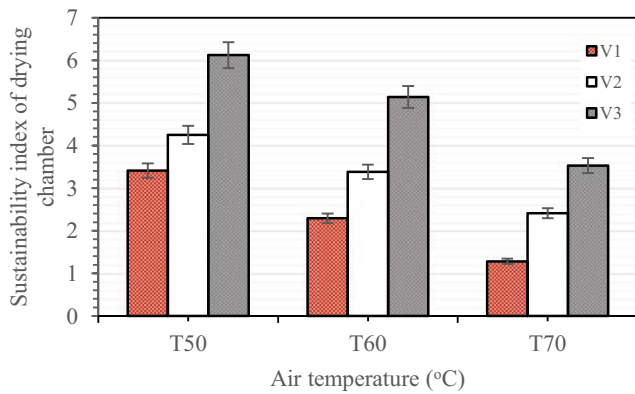
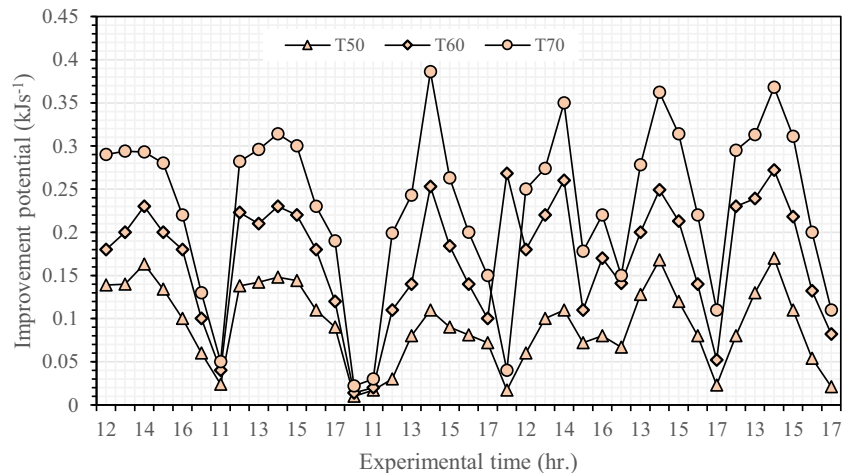


**Fig. 14** Exergetic sustainability index as affected by variations in air temperature and velocity of air

compartment is referred to as waste exergy ratio ( $E_w$ ) and calculated with Eq. (17) for the hybrid system. The influence of varying levels of air temperature and air flows (at uniform thickness of sample) on  $E_w$  is shown in Fig. 13. Higher exergy emanating from high temperature of the drying compartment at higher air velocity increases exergy loss to the ambient environment, hence increase in  $E_w$ . The waste exergy ratio varies between 0.11 and 0.167. These values are within the range of Ndukwu et al. (2017) for solar dryers.

Figure 14 illustratively presents the outcome of air temperatures and air flow rates on the exergetic sustainability index (Eq. 18), which is the amount of exergy emitted by the range of the studied parameters. At higher values of exergetic efficiency, which was prompted by decrease in temperature and increase in flow of air, the sustainability index ( $S^n$ ) increased, hence reduction in environmental impact (Ndukwu et al. 2020a, b, c). In other words,  $S^n$  value diminishes with temperature and increases with air flow. The values ranged from  $1.14 \leq S^n \leq 6.12$ . Ndukwu et al. (2017) obtained  $S^n$  values ranging between 3.01–8.15 for passive solar dryers; Beigi (2016) calculated values between 1.48–3.11 for deep bed convective drying of rice; Castro et al. (2018) reported  $S^n$  values

**Fig. 15** Variation of exergetic improvement potential with drying air temperature and time



of 1.9–5.1 for convective drying of onion. It is pertinent to remark that the peak  $S^n$ -value indicates a low environmental effect (Aghbashlo et al. 2013; Ndukwu et al. 2020a, Nwakuba et al. 2020). Therefore, in order to maintain a low environmental impact, exergy efficiency ought to be ameliorated. The results of this present study therefore, shows that supply of thermal energy at high temperature and airflow had no undermining consequence(s) on the environment nor possibility of uttering the environmental thermal equilibrium.

The influence of drying air temperature and experimental time on the improvement potential,  $P_{im}$  (Eq. 19) of sliced red pepper drying in a HHSD is detailed in Fig. 15. The improvement potential is a function of exergy efficiency which decreases with increasing air temperature and exergy loss, thus high improvement potential (Ndukwu et al. 2020a). In other words, the highest air temperature (70°C) gives an idea of where greater attention should be given for enhancement. It further implies that greater attention for improvement is needed in utilizing the thermal energy produced by the hybrid heat unit at 70°C air temperature and 14:00 hrs. During the insolation period, the  $P_{im}$ -values for this study varied between 0.021 and 0.386  $\text{kJ s}^{-1}$ . The gap between the first and last points on the curves indicate the scope for improvement in the drying system (Joshi et al. 2011). However, the effect of air velocity on  $P_{im}$  yielded no significant result. Similar observations were made by Castro et al. (2018) in onion drying and Aviara et al. (2014), who obtained  $P_{im}$ -values ranging between 0.02 and 0.76  $\text{kJ s}^{-1}$  for temperature range of 50–80°C. It is pertinent to state that the scope for improvement is relatively large in comparison to the  $P_{im}$  of solar dryers with thermal heat storage units (Ndukwu et al. 2017) and hybrid solar-biomass dryers (Ndukwu et al. 2020a, b, c).

### 3.7 Environmental Effect

The choice of a solar-electric (hybrid) heat source dryer is predicated on its high prospect for curbing carbon dioxide

emission to the atmosphere and sustaining drying operation at relatively low operational cost. Given the damp and humid nature of the environment for the experimental study, which concedes with the harvest season in the South-eastern Nigeria, the use of solar dryer and/or hybrid solar-biomass systems may not be quite promising as a result of poor insolation effect and greenhouse gas emission (like CO<sub>2</sub>) by the biomass heat unit, respectively. The quantity of fuel conserved from the CI engine-powered dryer that ought to have been expended to generate equal amount of energy utilized by both crop dryers was compared on the basis of degree of use. The mean annual price of quantity of diesel-fuel consumption is estimated at \$ 3, 359.86 (Eq. 24). However, the annual rate of operation of HHSD ranged between 0.1 and 1.0, and the estimated quantity of reduction in CO<sub>2</sub> emission is given in Fig. 16. A 3rd order polynomial function (Eq. 25) explains the drop in CO<sub>2</sub> emission ranging between 398.86 ≤ ε<sub>CO2</sub> ≤ 3872.7 tons, which were obtained annually at 10 and 100% operational periods, respectively. The correlation value (R<sup>2</sup> = 0.9995) substantiates robust relationship between ε<sub>CO2</sub> and rate of HHSD usage, as well as the aptitude of the polynomial function to clarify 99.95% variations in the reduction of CO<sub>2</sub> discharged at varying usage rates of the hybrid dryer. This result compared well with the reports of Ndukwu et al. (2020a) for hybrid solar-biomass dryer, with a higher CO<sub>2</sub> reduction potential of 30.25%. This demonstrates aptitude for gross reduction of atmospheric temperature and its attendant greenhouse effect therefore justifies the environmental sustainability of hybrid solar-electric dryer.

$$\begin{aligned} \epsilon_{\text{CO}_2} = & 0.0014x^3 - 0.121x^2 + 36.62x \\ & + 14.23 \quad [R^2 = 0.9995] \end{aligned} \quad (25)$$

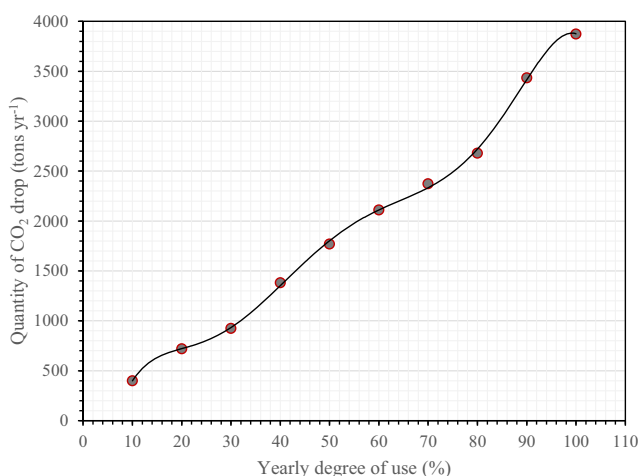


**Fig. 16** Estimated yearly reduced quantity of CO<sub>2</sub> from possible atmospheric emission

## 4 Conclusion

The environmental sustainability analysis of a hybrid solar crop dryer in humid Nigerian environment was undertaken. Considering the outcomes of this experimental study, the ensuing inferences are made:

During the experimental period, the solar intensity varied between 187 Wm<sup>-2</sup> to 892 Wm<sup>-2</sup>. The solar collector efficiency obtained ranged from 23.7 to 72.4%. The specific energy requirements for a batch of 500 g of red pepper slices in a hybrid solar dryer varied from 7.24 to 62.5 kJkg<sup>-1</sup>, respectively. Increasing the drying air temperature and air velocity at constant slice thickness reduces the specific energy requirements, whereas increase in slice thickness increases it. The percent solar energy contribution to the total energy requirement ranged between 28.8–52.68% at changing air temperatures (50, 60, and 70°C) and air velocities (1.14, 2.29, and 3.43 ms<sup>-1</sup>). The drying time varied between 75 ± 50 to 180 ± 24 min.

The energy utilization for drying of red pepper decreased with air velocity and slice thickness. Its values ranged between 176.95 Js<sup>-1</sup> and 3273.66 Js<sup>-1</sup>. The η<sub>e</sub> - value of HHSD improved 13.2–35.6% at process conditions of 50°C, 3.43 ms<sup>-1</sup>, 10 mm and 70°C, 1.14 ms<sup>-1</sup>, 20 mm, respectively; whereas exergy efficiency varied between 35.8–92.3%. The maximum (1.295 kJs<sup>-1</sup>) and minimum (0.327 kJs<sup>-1</sup>) exergy losses at constant slice thickness (10 mm) were obtained at 70°C air temperature, 3.43 ms<sup>-1</sup> air velocity, and 50°C air temperature, 1.41 ms<sup>-1</sup> air velocity, respectively. The waste exergy ratio varies between 0.11 ≤ E<sub>w</sub> ≤ 0.167, whereas the S<sup>n</sup> and P<sub>im</sub> -values are in the range of 1.14 ≤ S<sup>n</sup> ≤ 6.12 and 0.099 ≤ P<sub>im</sub> ≤ 0.289 kJs<sup>-1</sup>, respectively.

This study was able to achieve a 30.3% higher CO<sub>2</sub> reduction in comparison with that obtained from a hybrid solar-biomass dryer in an apparently similar climatic condition, with 398.86 to 3872.7 tons of carbon dioxide prevented from being emitted into the environment per annum. Based on the results obtained herein, there is no clear-cut merit of this methodology of analysis over the dynamic model approach adopted by few researchers, since the trend of all observational parameters are in agreement; except the numerical results that varied due to dryer structural differences, environmental effect, and crop sample handled. Therefore, future works may consider exergy sustainability analysis of hybrid solar-electric dryer based on the dynamic model in sub-tropical African climate. Optimization of the exergetic efficiency of the hybrid dryer for optimal improvement potential during the three major seasons in Nigeria is also recommended. Comparative analysis of the energetic and exergetic performance of solar cum electric dryer and other hybrid solar dryers using the proposed approaches should also be considered.

**Acknowledgements** Authors are thankful to the staff of Centre for Industrial Studies (CIS) Unit of the Federal University of Technology, Owerri, Nigeria.

## Compliance with Ethical Standards

**Conflict of Interest** Authors have no conflict of interest.

## References

- Afolabi TJ, Akintunde TY, Oyelade OJ (2014) Influence of drying conditions on the effective moisture diffusivity and energy requirements of ginger slices. *J Food Res* 3:103–112
- Aghbashlo M, Kianmehr MH, Arabhosseini A (2008) Energy and exergy analyses of thin-layer drying of potato slices in a semi-industrial continuous band dryer. *Dry Technol* 26:1501–1508
- Aghbashlo M, Mobli H, Rafiee S, Madadlou A (2013) A review on exergy analysis of drying processes and systems. *Renew Energy Rev* 22:1–22. <https://doi.org/10.1016/j.rser.2013.01.015>
- Akpinar EK (2004) Energy and exergy analyses of drying of red pepper slices in a convective type dryer. *Int Comm Heat Mass Transfer* 31:1165–1176. Available at: <https://www.sciencedirect.com>. Accessed 4 Feb 2020
- Akpinar EK (2011) Drying of parsley leaves in a solar dryer and under open sun: modeling, energy and exergy aspects. *J Food Process Eng* 34:27–48
- Alejandro R, Andrea M, Fracisco C, Pedro H (2013) Mushroom dehydration in a hybrid solar dryer. *Energy Convers Manag* 70:31–39
- Amer BMA, Hossain MA, Gottschalk K (2010) Design and performance evaluation of a new hybrid solar dryer for banana. *Energy Conv Manag* 51:813–820. <https://doi.org/10.1016/j.enconman.2009.11.016>
- Amer BMA, Gottschalk K, Hossain MA (2018) Integrated hybrid solar drying system and its drying kinetics of chamomile. *Renew Energy* 121:539–547
- Aviara NA, Onuoha LN, Falola OE, Igbeka JC (2014) Energy and exergy analyses of native cassava starch drying in a tray Dryer. *Energy* 73:809–817. <https://doi.org/10.1016/j.energy.2014.06.087>
- Azadbakht M, Torshizi VM, Ziaratban A, Aghili H (2017) Energy and exergy analysis during eggplant drying in a fluidized bed dryer. *Agric Eng Int* 19:177–182
- Beigi M (2016) Energy efficiency and moisture diffusivity of apple slices during convective drying. *Food Sci Technol* 36:145–150. <https://doi.org/10.1590/1678-457X0068>
- Bennamoun L (2012) An overview on application of exergy and energy for determination of solar drying efficiency. *Int J Energy Eng* 2:184–194. <https://doi.org/10.5923/j.ijee.20120205.01>
- Borah A, Sethi LN, Sarkar S, Hazarika K (2017) Drying kinetics of sliced turmeric (*curcuma longa l.*) in a solar- biomass integrated drying system. *J Food Process Preserv* 41(3):e12904
- Boughali S, Benmoussa H, Bouchekima B, Mennouche D, Bouguettaia H, Bechki D (2009) Crop drying by indirect active hybrid solar-electrical dryer in the eastern Algerian Septentrional Sahara. *Solar Energy* 83:2223–2232
- Castro M, Roman C, Echegaray M, Mazza G, Rodriguez R (2018) Exergy analyses of onion drying by convection: influence of dryer parameters on performance. *Entropy* 20:2–9
- Cheng F, Zhou X, Liu Y (2018) Methods for improvement of the thermal efficiency during spray drying: E3S Web of Conferences. 53, 1–3. <https://doi.org/10.1051/e3sconf/20185301031>
- Chowdhury MM, Bala BK, Haque MA (2011) Energy and exergy analysis of the solar drying of jackfruit leather. *Biosyst Eng* 110:222–229
- Darvishi H, Asi RA, Asghari A, Najafi G, Gazorix HA (2013) Mathematical modeling, moisture diffusion, energy consumption and efficiency of thin-layer drying of potato slices. *J Food Process Technol* 4:215–219
- Doymaz I (2004) Convective air drying characteristics for thin-layer carrots. *J Food Eng* 61(3):359–364
- Dincer I, Rosen MA (2013) Exergy, energy, environment and sustainable development. Elsevier Ltd, Oxford
- El-Ferouali H, Zoukit A, Salhi I, El Kilali T, Doubabi S, Abdenouri N (2019) Optimization study and design of a hybrid solar-electric dryer suitable to the developing countries context. *Solar Afr Renew Energy J* 1(19):35–39
- Erbay Z, Icier F (2011) Energy and exergy analysis on drying of olive leaves (*oleaeuropaca L.*) in tray drier. *J Food Process Eng* 34:2105–2123
- Eltawil MA, Azam MM, Alghannam AO (2018) Energy analysis of hybrid solar tunnel dryer with PV system and solar collector for drying mint (*MenthaViridis*). *J Clean Prod* 181:352–364
- Fu M, Roman C, Echegaray M, Mazza G, Rodriguez R (2018) Exergy analyses of onion drying by convection: influence of dryer parameters on performance. *Entropy* 20:2–9. <https://doi.org/10.3390/e20050310>
- Fudholi A, Yendra R, Basri DF, Ruslan MH, Sopian K (2016) Energy and exergy analysis of hybrid solar drying system. *Cont Eng Sci* 9:215–223. <https://doi.org/10.12988/ces.2016.512323>
- Hatami S, Payehaneh G, Mehrpanahi A (2019) Energy and exergy analysis of an indirect solar dryer based on a dynamic model. *J Clean Prod*. <https://doi.org/10.1016/j.jclepro.2019.118809>
- Hossain MZ, Alam MM, Hossain MF, Sarker MS (2018) Performance evaluation of a cabinet solar dryer for drying red pepper in Bangladesh. *J Agric Eng* 774:100–109
- Jamil B, Bellos E (2019) Development of empirical models for estimation of global solar radiation exergy in India. *J Clean Prod* 207:1–16
- Joshi AS, Dincer I, Reddy B (2011) Analysis of energy and exergy efficiencies for PV/T systems. *Int J Low Carbon Technol* 6:64–69. <https://doi.org/10.1093/ijlct/ctq045>
- Maia CB, Kumar D, Prasad S, Murthy GS (2017) Optimization of microwave-assisted hot air drying conditions of okra using response surface methodology. *J Food Sci Technol* 4:1–13
- Lamidi RO, Jiang L, Pathare PB, Wang Y, Roskilly AP (2019) Recent advances in sustainable drying of agricultural produce: A review. *Appl Energy* 233:367–385
- Lamrani B, Khouya A, Draoui A (2019) Energy and environmental analysis of an indirect solar dryer of wood using TRNSYS software. *Sol Energy* 183:132–145
- Lopez-Vidana EC, Mendez-Lagunas LL, Rodriguez-Ramirez J (2013) Efficiency of a hybrid solar-gas dryer. *Sol Energy* 93:23–31. <https://doi.org/10.1016/j.solener.2013.01.027>
- Midilli A, Kucuk H (2014) Exergy-based sustainability indicators for a single layer solar drying process. *Progress Exerg Energ Env* 3:705–712. [https://doi.org/10.1007/978-3-319-04681-5\\_67](https://doi.org/10.1007/978-3-319-04681-5_67)
- Minaei S, Chenarbon HA, Motevali A, Arabhosseini A (2014) Energy consumption, thermal utilization efficiency and hypericin content in drying leaves of St&nbsp;John’s Wort (*Hypericum Perforatum*). *J Energy S Afr* 25:27–35
- Motevali A, Abbaszadeh A, Minaei S, Khoshtaghaza MH, Ghobadian B (2012) Effective moisture diffusivity, activation energy and energy consumption in thin-layer drying of jujube (*Zizyphus jujube Mill*). *J Agric Sci Technol* 14:523–532
- Nazghelichi T, Kianmehr MH, Aghbashlo M (2010) Thermodynamic analysis of fluidized bed drying of carrot cubes. *Energy* 35:4679–4684
- Ndukwu MC, Bennamoun L, Abam FI, Eke AB, Ukoha D (2017) Energy and exergy analysis of a solar dryer integrated with sodium sulfate decahydrate and sodium chloride as thermal storage medium.

- Renew Energy 113:1182–1192. <https://doi.org/10.1016/j.renene.2017.06.097>
- Ndukwu MC, Bennamoun L, Anozie O (2018a) Evolution of thermo-physical properties of *Akuama* (*picralima nitida*) seed and antioxidants retention capacity during hot air drying. *Sol Energy* 54:3533–3546
- Ndukwu MC, Bennamoun L, Abam FI (2018) Experience of solar drying in Africa: presentation of designs, operations, and models. *Food Eng Rev* 10:211e244. <https://doi.org/10.1007/s12393-018-9181-2>
- Ndukwu MC, Simo-Tagne M, Abam FI, Onwuka OS, Prince S, Bennamoun L (2020a) Exergetic sustainability and economic analysis of hybrid solar-biomass dryer integrated with copper tubing as heat exchanger. *Heliyon* 6(2020):e03401. <https://doi.org/10.1016/j.heliyon.2020.e03401>
- Ndukwu MC, Onyenwigwe D, Abam FI, Eke AB, Dirioha C (2020b) Development of a low-cost wind-powered active solar dryer integrated with glycerol as thermal storage. *Renewable Energy* (2020) <https://doi.org/10.1016/j.renene.2020.03.016>
- Ndukwu MC, Simo-Tagne M, Bennamoun L (2020c) Solar drying research of medicinal and aromatic plants: An African experience with assessment of the economic and environmental impact. *African Journal of Science, Technology, Innovation and Development*. <https://doi.org/10.1080/20421338.2020.1776061>
- Nwajinka CO, Onuegbu CU (2014) Development of a solar cabinet dryer for root crops chips in Nigeria. *J Agric Eng Tech* 22:47–58
- Nwakuba NR, Asoegwu SN, Nwaigwe KN (2016) Energy consumption of agricultural dryers: an overview. *Agric Eng Int CIGR* 18:119–132
- Nwakuba NR, Asoegwu SN, Nwaigwe KN, Chukwuezie OC (2017) Design and development of a hybrid solar-electric dryer for sliced vegetable crops. *J Agric Eng Tech* 2:48–64
- Nwakuba NR, Chukwuezie OC, Asonye GU, Asoegwu SN (2018) Energy analysis and optimization of thin layer drying conditions of okra. *Arid Zone J Eng Tech Env* 14:135–154
- Nwakuba NR, Okafor VC, Okorafor OO (2020) Techno-economic analysis of a hybrid solar-electric dryer. *Energy Sour A Recover Utilization Environ Eff*. <https://doi.org/10.1080/15567036.2020.1782537>
- Nwofe PA (2014) Utilization of solar and biomass energy- a panacea to energy sustainability in a developing economy. *Int J Electron Eng Res* 2(3):10e19
- Okoroigwe EC, Eke MN, Ugwu HU (2013) Design and evaluation of combined solar and biomass dryer for small and medium enterprises for developing countries. *Int J Phy Sci* 8:1341–1349
- Ould-Amrouche S, Rekioua D, Hamidat A (2010) Modelling photovoltaic water pumping systems and evaluation of their CO<sub>2</sub> emissions mitigation potential. *Appl Energy* 87:3451–3459
- Reyes A, Mahn A, Huenulaf P, Gonzalez T (2014) Tomato dehydration in a hybrid solar dryer. *Chem Eng Pro Tech* 5:1–8
- Rosen MA, Dincer I, Kanoglu M (2008) Role of exergy in increasing efficiency and sustainability and reducing environmental impact. *Energy Policy* 36:128–137. <https://doi.org/10.1016/j.enpol.2007.09.006>
- Shamekhi-Amiri S, Gorji TB, Gorji-Bandpy M, Jahanshahi M (2018) Drying behaviour of lemon balm leaves in an indirect double-pass packed bed forced convection solar dryer system. *Case Stud Therm Eng* 12:677–686
- Silva GM, Ferreira AG, Coutinho RM, Maia CB (2020) Experimental analysis of corn drying in a sustainable solar dryer. *J Adv Res in Fluid Mech Therm Sci* 67(2):1–12
- Sansaniwal SK, Sharma V, Mathur J (2018) Energy and exergy analyses of various typical solar energy applications: a comprehensive review. *Renew. Sustain. Energy Rev.* 82 (2018):1576e1601
- Tiwari GN (2012) *Solar Energy Fundamentals, Design, Modeling and Application*. Narosa Publishing House PVT Ltd., New Delhi, pp 203–250
- Uzoma S, Nwakuba NR, Anyaoha K (2020) Response surface optimization of convective air drying process in a hybrid PV/T solar dryer. *Turk J Agric Eng Res* 1(1):111–130

**Publisher's Note** Springer Nature remains neutral with regard to jurisdictional claims in published maps and institutional affiliations.